



A novel fluorescent bisazomethine dye derived from 3-hydroxyquinoxaline-2-carboxaldehyde and 2,3-diaminomaleonitrile

V. Arun, P.P. Robinson, S. Manju, P. Leeju, G. Varsha, V. Digna, K.K.M. Yusuff*

Department of Applied Chemistry, Cochin University of Science and Technology, Cochin 682 022, Kerala, India

ARTICLE INFO

Article history:

Received 26 November 2008

Received in revised form

9 January 2009

Accepted 18 January 2009

Available online 29 January 2009

Keywords:

3-Hydroxyquinoxaline-2-carboxaldehyde

2,3-Diaminomaleonitrile

Schiff base

Solvatochromism

Fluorescence

Cyclic voltammetry

ABSTRACT

A novel bisazomethine Schiff base was synthesised by the condensation of 3-hydroxyquinoxaline-2-carboxaldehyde and 2,3-diaminomaleonitrile. ^1H NMR, ^{13}C NMR, HPLC and FT-IR studies revealed that the compound exists in two major tautomeric forms. The Schiff base exhibits positive absorption and fluorescent solvatochromism and displays dual fluorescence with large stoke shifts. Cyclic voltammetric analysis of the compound in 1:1 methanol-THF was influenced by scan rate. Thermal analysis of the compound was undertaken using TG-DTA and DSC.

© 2009 Elsevier Ltd. All rights reserved.

1. Introduction

Quinoxalines represent an important class of nitrogen-containing heterocycles and have gained increasing attention in recent years due to their different applications in various areas. They find applications as dyes [1–3], as fluorescent materials [4–6] and as organic light emitting devices [7–13]. Quinoxaline derivatives exhibit a broad spectrum of biological activities [14,15] and find place in the chemical libraries for DNA binding [16,17].

Azomethine dyes derived from diaminomaleonitrile are also found to have application in the field of dyes [18,19]. Azomethine dyes are commonly used in colour photography [20]. The inherent characteristic properties of dye molecules are strongly dependent on the intermolecular charge-transfer interactions involving π -electrons and intramolecular π - π interactions of the dye chromophore [21]. It was therefore considered worthwhile to synthesise a new azomethine dye through the interaction of 3-hydroxyquinoxaline-2-carboxaldehyde and 2,3-diaminomaleonitrile. In this paper we report a detailed investigation on the synthesis, thermal, ^1H NMR, ^{13}C NMR, UV-vis, FT-IR, HPLC analyses, cyclic voltammetric and fluorescent studies of a new bisazomethine dye.

2. Experimental

2.1. Materials

All the chemicals were obtained from Sigma-Aldrich Chemicals, India and were used as supplied. Solvents used were purified and dried using standard methods.

2.2. Methods

Microanalyses of the compounds were done with an Elementar Vario EL III CHNS elemental analyzer. Room-temperature FT-IR spectra were recorded as KBr pellets with a JASCO FTIR 4100 Spectrophotometer in the 4000–400 cm^{-1} range. The electronic spectra of the Schiff base in different solvents were recorded on a Thermo Electron Nicolet Evolution 300 UV-vis Spectrophotometer. The UV-vis Diffuse Reflectance spectra were recorded on a Labomed UV-vis spectrophotometer equipped with a diffuse reflectance accessory in the range 200–900 nm. The percentage reflectance values were converted to absorbance using the Kubelka Munk function. ^1H NMR and ^{13}C NMR spectra of all the synthesised compounds were recorded in DMSO- d_6 on a Bruker Avance DRX 500 MHz NMR spectrometer. The fluorescence spectra of the compound in different solvents were recorded on a Cary Eclipse Fluorescence Spectrophotometer (Varian). TG-DTA analysis was carried out under air and nitrogen with a heating rate of

* Corresponding author. Tel.: +91 484 2575804.

E-mail address: yusuff@cusat.ac.in (K.K.M. Yusuff).

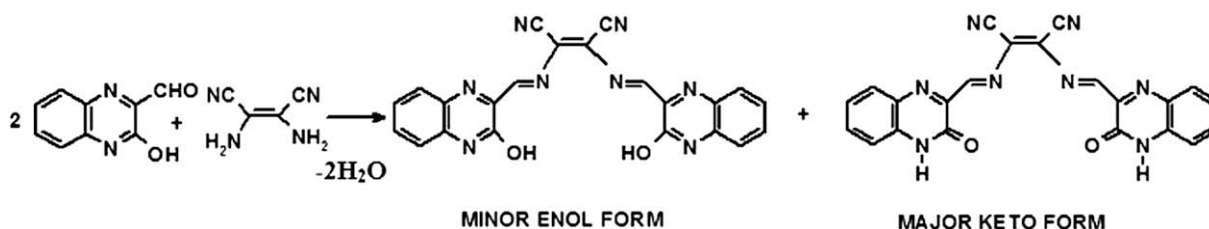


Fig. 1. Synthesis of hqcdmn.

20 °C min⁻¹ using a Perkin Elmer Pyres Diamond TG/DTA analyser. DSC analysis was carried out using a Mettler Toledo DSC 822e. Cyclic voltametric studies were carried out with a BAS EPSILON Electrochemical Analyser using glassy-carbon working electrode. A Pt wire and Ag/AgCl were used as counter and reference electrodes, respectively.

The HPLC analysis was performed on a Dionex UltiMate 3000 HPLC system equipped with UltiMate 3000 Pump, UltiMate 3000 Autosampler Column Compartment, UltiMate 3000 Photodiode Array Detector and Chromeleon software. Separation was carried out using an Acclaim[®] 120 column, C18 5 μm 120 Å (4.6 × 250 mm), with a guard column packed with the same material. The column was maintained at 30 °C throughout the analysis and the detection was at 254 nm. HPLC grade acetonitrile and water (Qualigens) were used for sample preparation and for mobile phase. The mobile phase used was 70% acetonitrile–water with a flow rate of 1 mL/min.

2.3. Synthesis of Schiff base

The synthesis of the Schiff base involved two main stages namely synthesis of 3-hydroxyquinoxaline-2-carboxaldehyde and the subsequent condensation of this aldehyde with 2,3-diaminomaleonitrile.

2.3.1. Synthesis of 3-hydroxyquinoxaline-2-carboxaldehyde (hq)

The synthesis of the aldehyde involves preparation of 3-hydroxy-2-methylquinoxaline, 3-hydroxy-2-dibromomethylquinoxaline and subsequent conversion of the latter to the aldehyde.

2.3.1.1. Preparation of 3-hydroxy-2-methylquinoxaline (hmq). Separate solutions of orthophenylenediamine (10.8 g, 100 mmol) and sodium pyruvate (11.0 g, 100 mmol) in 250 mL distilled water were prepared. The sodium pyruvate solution was converted to pyruvic acid using conc. HCl (8 mL) and the ensuing solution was

transferred to 1 L beaker to which was added, orthophenylenediamine, drop-wise, with constant stirring. The precipitated pale yellow coloured compound was filtered, washed with water and dried over anhydrous calcium chloride. The crude sample was recrystallised from 50% absolute ethanol. Yield: (90%, 14.4 g); colour: pale yellow; no sharp melting point. The compound decomposes within the range 212–225 °C accompanied by a change in colour from pale yellow to light brown.

Anal. Calcd. for C₉H₈N₂O (160.17): C, 67.49; H, 5.03; N, 17.49. Found: C, 67.38; H, 4.98; N, 17.37. IR (cm⁻¹): 3313, 3168, 3108, 3011, 2966, 2900, 2845, 2784, 2707, 1950, 1920, 1666, 1611, 1569, 1504, 1486, 1431, 1381, 1350, 1279, 1213, 1192, 1158, 1117, 1030, 1010, 974, 945, 929, 892, 852, 779, 755, 728, 692, 601, 585, 560, 468, 455, 416. λ_{max} (nm) in methanol (10⁻⁴ mol L⁻¹) = 210, 229, 278, 335; ε_{max} (L mol⁻¹ cm⁻¹) = 2.98 × 10⁴, 3.51 × 10⁴, 0.94 × 10⁴, 1.13 × 10⁴. ¹H NMR δ p.p.m.: (500 MHz, DMSO-*d*₆, 295 K): δ = 2.40 (s, 3H, C-CH₃), 7.28, 7.27, 7.25 (t, 1H), 7.45, 7.46 (d, 1H), 7.47, 7.48, 7.49 (t, 1H), 7.69, 7.70 (d, 1H), 12.31 (s, 1H, Ar-OH or N-H). ¹³C NMR (500 MHz, DMSO-*d*₆, 296 K) δ p.p.m.: 159.17, 154.88, 131.88, 131.61, 129.26, 127.82, 122.98, 115.17, 20.48.

2.3.1.2. Preparation of 3-hydroxy-2-dibromomethylquinoxaline (hdmq). To a solution of 3-hydroxy-2-methylquinoxaline (16.0 g, 100 mmol) in glacial acetic acid (200 mL), 10% (v/v) bromine in glacial acetic acid (110 mL) was added with stirring. The mixture was then exposed to sunlight for 1 h with occasional stirring and then was diluted to 1 L using distilled water and the precipitated dibromo compound was filtered, washed with water and dried. The crude product was purified by recrystallisation 50% absolute ethanol. Yield: (92%, 29.3 g); colour: pale yellow; no sharp melting point, but decomposes within the range 210–222 °C with a change in colour from pale yellow to light brown.

Anal. Calcd. for C₉H₆Br₂N₂O (317.96): C, 34.00; H, 1.90; N, 8.81. Found: C, 33.93; H, 1.86; N, 8.77. IR (cm⁻¹): 3314, 3156, 3104, 3009, 2969, 2888, 2836, 2775, 2715, 1662, 1612, 1557, 1502, 1480, 1433,

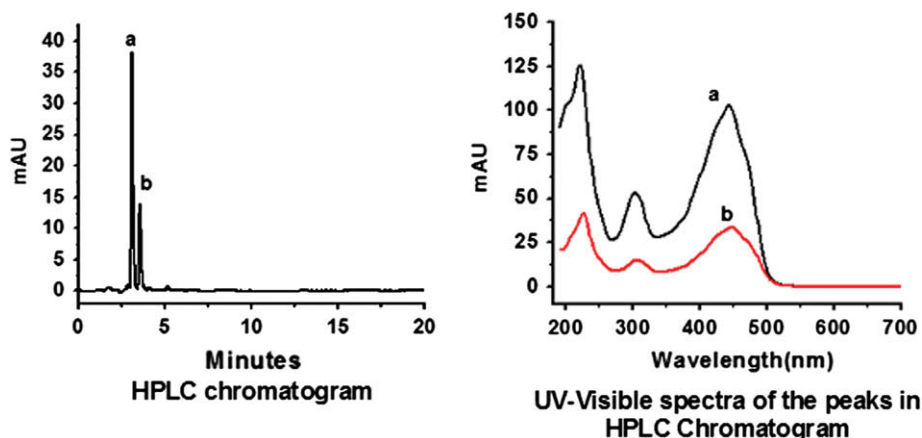


Fig. 2. HPLC chromatogram of hqcdmn in acetonitrile and UV-visible spectra of the peaks.

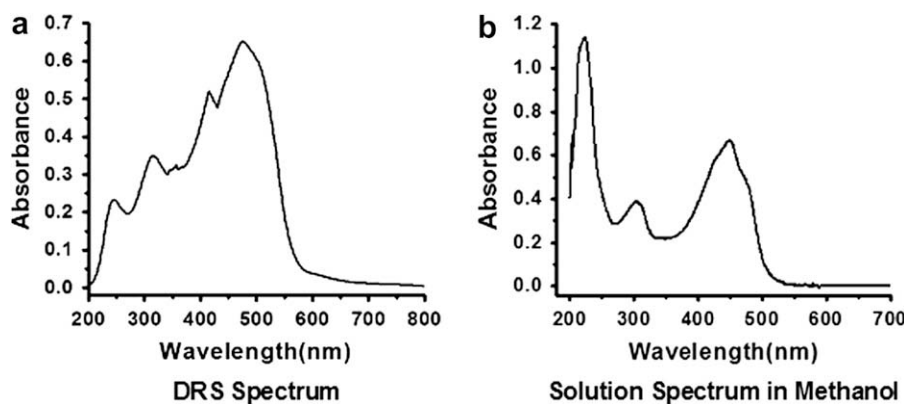


Fig. 3. The DRS (a) and solution spectra (b) of hqcdmn.

1398, 1350, 1281, 1225, 1158, 1131, 1103, 1069, 1022, 956, 943, 913, 895, 866, 825, 799, 761, 734, 714, 684, 618, 601, 563, 502, 476, 468, 447, 431. λ_{\max} (nm) in methanol (10^{-4} mol L $^{-1}$) = 212, 232, 296, 359; ϵ_{\max} (L mol $^{-1}$ cm $^{-1}$) = 2.98×10^4 , 2.65×10^4 , 1.04×10^4 , 0.98×10^4 . ^1H NMR δ p.p.m.: (500 MHz, DMSO- d_6 , 295 K): δ = 7.25 (s, 1H, CH-Br $_2$), 7.37, 7.38, 7.39 (t, 1H), 7.51, 7.53 (d, 1H), 7.61, 7.62, 7.63 (t, 1H), 7.85, 7.84 (d, 1H), 10.18 (s, 1H, Ar-OH or N-H). ^{13}C NMR (500 MHz, DMSO- d_6 , 297 K) δ p.p.m.: 154.21, 151.23, 136.57, 131.87, 130.86, 128.96, 123.95, 115.61, 29.62.

2.3.1.3. Preparation of 3-hydroxyquinoxaline-2-carboxaldehyde (hqc). The dibromo compound (5 g, 15.7 mmol) was thoroughly mixed with precipitated calcium carbonate (20 g) using a mortar and pestle. The ensuing mixture was refluxed with distilled water (500 mL) for 3 h with occasional shaking and the aldehyde remaining in solution was collected by filtration. The yellow coloured aqueous solution thus obtained was very stable and could be used for the preparation of Schiff base. The aldehyde was obtained as a fine yellow powder by concentrating the aqueous solution using rotary evaporation, extracting the aldehyde with ether, drying the ether extract with anhydrous sodium sulphate and removal of ether with rotary evaporation.

Colour: yellow; no sharp melting point. The aldehyde decomposes within the range 108–130 °C and the colour is changed from yellow to light brown. The yellow solid is not stable and changes its colour to light brown in air indicating oxidation/decomposition of the aldehyde. However the aqueous solution of the aldehyde is

stable. Therefore, it would be better to use the aldehyde solution for the synthesis of Schiff base.

Yield (solid aldehyde): (51%, 1.4 g). Anal. Calcd. for C $_9$ H $_6$ N $_2$ O $_2$ (174.16): C, 62.07; H, 3.47; N, 16.09. Found: C, 62.01; H, 3.40; N, 16.06. IR (cm $^{-1}$): 3483, 3164, 3095, 3012, 2965, 2906, 2836, 1721, 1670, 1600, 1568, 1541, 1497, 1420, 1394, 1345, 1260, 1218, 1160, 1072, 1025, 942, 900, 872, 825, 807, 762, 722, 647, 607, 587, 548, 526, 483, 432. λ_{\max} (nm) in methanol (10^{-4} mol L $^{-1}$) = 209, 231, 283, 338; ϵ_{\max} (L mol $^{-1}$ cm $^{-1}$) = 2.78×10^4 , 2.17×10^4 , 0.67×10^4 , 0.75×10^4 . ^1H NMR δ p.p.m.: (500 MHz, DMSO- d_6 , 296 K): δ = 7.28–7.92 (m, 4H, aromatic quinoxaline ring), 10.25 (s, 1H, -CH=O), 12.40–13.00 (m, 1H, Ar-OH or N-H). ^{13}C NMR (500 MHz, DMSO- d_6 , 297 K) δ p.p.m.: 188.88, 160.00, 153.89, 149.36, 134.37, 133.15, 131.75, 130.50, 115.51.

2.3.2. Synthesis of N,N'-bis(3-hydroxyquinoxaline-2-carboxalidene)2,3-diaminomaleonitrile (hqcdmn)

To a solution of 3-hydroxyquinoxaline-2-carboxaldehyde (5 g, 28.7 mmol, in 500 mL distilled water), 3–4 drops of conc. HCl was added. An alcoholic solution of 2,3-diaminomaleonitrile (1.6 g,

Table 1
UV-visible absorption spectra of hqcdmn in different solvents.

Solvent	λ_{\max} (nm) ($\epsilon_{\max} \times 10^{-5}$ (L mol $^{-1}$ cm $^{-1}$))
Ethanol	206 (1.39); 223 (1.19); 303 (0.43); 451 (0.79)
Methanol	223 (1.14); 302 (0.39); 448 (0.67)
Isopropyl alcohol	215 (2.12); 253 (0.31); 262 (0.31); 268 (0.27); 304 (0.22); 453 (0.45); 482 ^a (0.31)
Ethyl acetate	251 (0.36); 299 (0.32); 446 (0.54)
Acetonitrile	206 (2.31); 301 (0.36); 440 (0.66)
Tetrahydrofuran	240 (0.32); 301 (0.28); 445 (0.55)
Dichloromethane	228 (0.26); 262 (0.23); 268 (0.19); 301 (0.07); 444 (0.12)
Dimethylformamide	269 (0.30); 303 (0.35); 360 (0.35); 448 (0.46); 509 ^a (0.25)
Dimethylsulphoxide	257 (0.51); 269 (0.45); 305 (0.53); 439 (0.83); 543 ^a (0.13)
Methanol-water (1:6) containing NaOH	192 (1.03); 207 (1.10); 227 (1.16); 305 (0.44); 367 ^a (0.36); 454 (0.63)
DRS	246, 315, 415, 476

^a Refers to the shoulder peak.

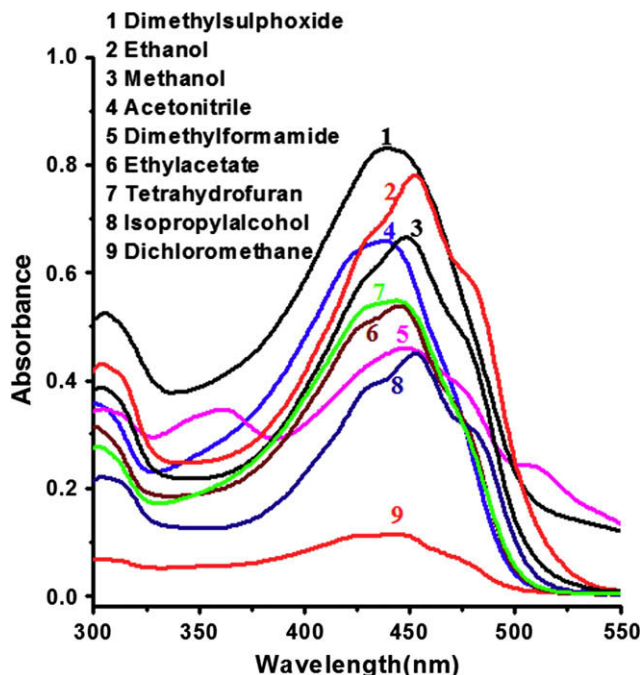


Fig. 4. The UV-visible spectra of hqcdmn in various solvents in the range 300–550 nm.

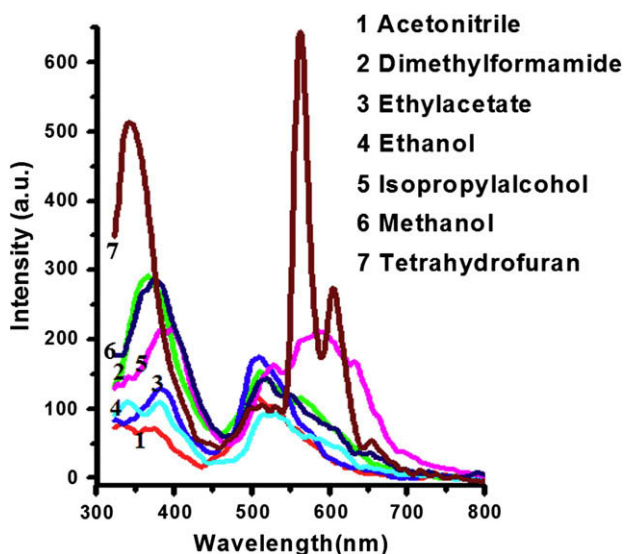


Fig. 5. Photoluminescence spectra of hqcdmn in various solvents at the excitation wavelength 302 nm.

14.4 mmol) in methanol (20 mL) was added to this solution dropwise with constant stirring. The red coloured Schiff base (Fig. 1) was filtered, washed with water and dried over anhydrous calcium chloride. The crude product was recrystallised from absolute ethanol.

Yield: (90%, 5.9 g). Anal. Calcd. for $C_{22}H_{12}N_8O_2$ (420.38): C, 62.86; H, 2.88; N, 26.66. Found: C, 62.78; H, 2.72; N, 26.42. IR (KBr, ν cm^{-1}): 3390, 3168, 3100, 2960, 2914, 2846, 2789, 2709, 2243, 2202, 1674, 1643, 1606, 1598, 1557, 1509, 1493, 1468, 1432, 1392, 1376, 1349, 1328, 1288, 1266, 1220, 1153, 1119, 1070, 1024, 949, 923, 904, 847, 821, 786, 753, 714, 702, 673, 654, 628, 611, 593, 570, 554, 524, 509, 480, 406. 1H NMR (500 MHz, DMSO- d_6 , 298 K) δ p.p.m.: 7.86–7.26 (aromatic protons), 8.98–8.53 (m, 2H, azomethine proton), 12.77, 12.67 (Ar–OH or N–H). ^{13}C NMR (500 MHz, DMSO- d_6 , 298 K) δ p.p.m.: 192.22, 161.62, 155.29, 148.37, 141.22, 133.52, 131.20, 129.41, 126.32, 123.96, 115.61.

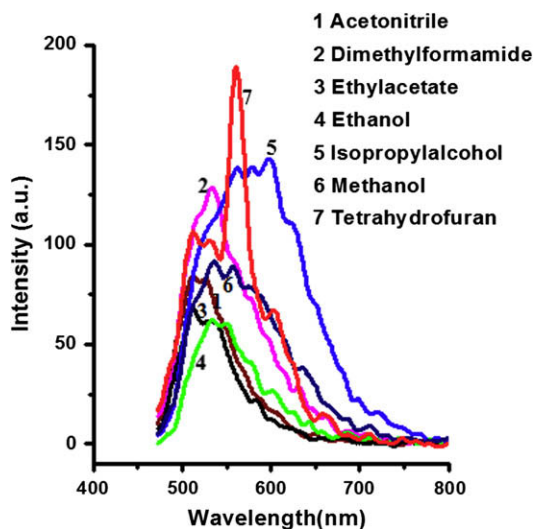


Fig. 6. Photoluminescence spectra of hqcdmn in various solvents at the excitation wavelength 450 nm.

3. Results and discussion

Extensive spectroscopic investigations have been reported on 2-hydroxyquinoxalines and their derivatives; but these investigations are mainly centred on their prototropic equilibrium [22,23]. This amide–iminol tautomerism involves a fast hydrogen transfer between nitrogen and oxygen and these compounds usually exist in the predominant amide form [24–30].

3.1. Infrared spectrum

The IR spectrum of the hqcdmn shows one strong absorption band around 3390 cm^{-1} which is either due to a hydrogen bonded $\nu_{(OH)}$ in the iminol tautomer or $\nu_{(NH)}$ in the amide tautomer. The medium intensity bands observed in the range $3100\text{--}2709\text{ cm}^{-1}$ may be due to the asymmetric and symmetric stretching vibrations of the aromatic CH groups [31]. In the case of tautomeric quinoxaline derivatives, particularly quinoxaline-2-ones, the IR stretching frequencies of the C=O and C=N (quinoxaline ring) vary from compounds to compounds. It is not easy to assign a particular range for these two types of stretching frequencies. The IR stretching frequencies of C=O and C=N (quinoxaline ring) of a series of 4-oxo-1-phenyl-4,5-dihydroimidazo[1,5-a]quinoxalines fall in the range $1700\text{--}1660\text{ cm}^{-1}$ and $1605\text{--}1610\text{ cm}^{-1}$ respectively [32]. Mamedov and co-workers prepared a series of quinoxaline-2-ones and found that the stretching frequencies of C=O and C=N (quinoxaline ring) lie in the range $1680\text{--}1665\text{ cm}^{-1}$ and $1625\text{--}1600\text{ cm}^{-1}$ respectively [26,28,33].

In the amide tautomeric form, the molecule contains two ketonic groups attached to each quinoxaline ring. The peaks observed at 1674 cm^{-1} may be due to the C=O group of the amide tautomer of the Schiff base. The IR spectrum of hqcdmn may be easily fingerprinted by two very intense $\nu_{(C\equiv N)}$ bands at 2243 and 2202 cm^{-1} . Although hqcdmn contains different types of C=N bonds, they were not well resolved in the infrared spectrum of the hqcdmn. The azomethine $\nu_{(CH=N)}$ band is superimposed with the C=O group of the amide tautomer and appears as a weak band at 1643 cm^{-1} . The $\nu_{(C=N)}$ stretch of the quinoxaline ring is observed at 1598 cm^{-1} . The $\nu_{(C=N)}$ (azomethine) falls in between $\nu_{(C=O)}$ group of the amide tautomer and the $\nu_{(C=N)}$ of the quinoxaline ring. A group of band observed in the range $1220\text{--}923\text{ cm}^{-1}$ may be due to the aromatic in-plane deformation vibrations.

3.2. NMR spectrum

The 1H NMR spectrum of hqcdmn in DMSO- d_6 shows signals confirmed with the tautomeric structure. The peaks at 12.77 and 12.67 ppm are assignable to the proton of the N–H of the amide tautomer or O–H of the iminol form of hqcdmn [34]. The azomethine protons appear as multiplets in the range 8.98–8.53 ppm. Multiplet signals observed at 7.86–7.26 ppm range are due to the aromatic protons of the hqcdmn.

3.3. HPLC analysis

The HPLC analysis of the hqcdmn in acetonitrile ($10^{-4}\text{ mol L}^{-1}$) reveals that the compound may exist in two forms. The HPLC chromatogram (Fig. 2) gave two peaks, with retention times 3.10 min (a) with relative area percentage of 71.4 and 3.55 min (b) with the relative area percentage of 28.6 indicating that the compound exists in two forms. For the peak, a, the absorption occurs at 201 (shoulder), 221, 303 and 443 nm and for b, they are at 226, 306 and 448 nm. The electronic spectrum of the species corresponding to the major peak is due to the amide form and that corresponding to the minor peak is the iminol form.

Table 2
Fluorescence spectral data and stokes shift of hqcdmn in various solvents.

Solvent	Fluorescence ^a (nm)	Fluorescence ^b (nm)	Wavelength ^d (nm)	Stokes shift ^a (nm)	Stokes shift ^b (nm)
Ethanol	340, 384, 515, ^c 530	535, ^c 550	451	64	84
Methanol	374, 519, ^c 550	536, ^c 557	448	71	88
Isopropyl alcohol	381, 398, 530, 586, ^c 634	562, 578, 598 ^c	453	133	145
Ethyl acetate	381, 510 ^c	512, ^c 532	446	64	66
Acetonitrile	331, 371, 505, ^c 533	512, ^c 527	440	65	72
Tetrahydrofuran	342, 512, 563, ^c 605	512, 531, 560 ^c	445	118	115
Dimethylformamide	367, 512, ^c 564	535 ^c	448	64	87

^a Excitation at 302 nm.

^b Excitation at 450 nm.

^c Fluorescent maxima.

^d Longest wavelength of absorption.

3.4. Electronic spectrum

The diffuse reflectance spectrum (DRS) of hqcdmn shows bands at 246, 315, 415 and 476 nm. The first one is due to the $\pi \rightarrow \pi^*$ transitions of the heterocyclic quinoxaline ring and the second one is due to the $n \rightarrow \pi^*$ transition of the $-C=N-$ group in quinoxaline ring [35]. The azomethine $n \rightarrow \pi^*$ transition appears at 476 nm. All the absorption peaks are blue shifted in methanol with respect to the peaks in the DRS spectrum. The solid state DRS and optical absorption spectrum in methanol ($10^{-5} \text{ mol L}^{-1}$) of the hqcdmn are shown in Fig. 3.

In solution, the ground state of hqcdmn is stabilised by hydrogen bonding with the solvent. In the excited state, the hydrogen bond of the molecule is almost completely broken or weakened to a larger extent. As a result the excited state is less stabilised and absorption is shifted to higher energy [36,37]. Similar trend was observed in the case of all other solution spectra.

The UV–vis spectra of the hqcdmn in various solvents with different polarities were taken and their intensities and wavelengths of absorption maximum are reported in Table 1. Fig. 4 shows the UV–visible spectra of hqcdmn in various solvents in the range 300–550 nm. The values of the longest wavelength absorption band of hqcdmn in various solvents are found to be increased with increasing solvent polarity. This positive solvatochromism exhibited by the compound may be due to the effect of dipole moment changes of the excited state, changes in the hydrogen bonding strength and/or due to excited state protonation [36,37]. The enolate anion, formed by the dissolution of hqcdmn in an equivalent amount of NaOH, in 1:6 methanol–water mixtures absorbs at a higher wavelength compared to the non-enolate form [38,39].

3.5. Fluorescence studies

The photoluminescence spectra of hqcdmn in $10^{-4} \text{ mol L}^{-1}$ solution in various solvents at two different excitation wavelengths (302 and 450 nm) were recorded and are not identical (Figs. 5 and 6).

Table 3
Electrochemical data of hqcdmn in methanol–tetrahydrofuran.

Scan rate (V)	Anodic peak potential (E_{pc} , mV)	Cathodic peak potential (E_{pa} , mV)	Anodic peak current (I_{pc} , μV)	Cathodic peak current (I_{pa} , μV)	No. of electrons (I_{pc}/I_{pa})
50	112	344; -898	4.17	3.79	1.10
100	-5	353; -769	17.58	15.87	1.11
150	-64	383; -717	23.61	22.93	1.03
200	-181; -355	410; -656	26.96	21.99	1.22
250	-396	388; -662	43.66	2.32	2.32
300	-437	377; -623	51.04	21.22	2.40

At the excitation wavelength 302 nm hqcdmn exhibits dual fluorescence with two well resolved fluorescence bands in the range 331–398 nm and 505–634 nm in all solvents (Table 2). The dual emission of fluorescent spectra may be due to excited state proton transfer nature of the hqcdmn [40]. The relative intensities of the long wavelength emission and short wavelength emission are strongly dependent on the nature of the solvent. For the excitation at 450 nm we can see fluorescent bands with peak splitting in the range 512–598 nm (Fig. 6 and Table 2).

The emission maximum is shifted to longer wavelength in more polar solvents, thus exhibiting a positive fluorescent solvatochromism, which indicates that the molecules become more polar in the excited states than in the ground state. The stokes shift in various solvents was seen to vary in the range 64–145 nm (Table 2). The large stokes shift for the present case may be either due to its less rigid structure or due to significant molecular rearrangement, that takes place upon photoexcitation [41]. The stokes shift increases with increasing solvent polarity.

3.6. Cyclic voltammetry

The electrochemical behaviour of the Schiff base has been investigated in 1:1 mixture of methanol–THF (Table 3). The cyclic voltammograms of hqcdmn with six different scans were recorded and are shown in Fig. 7. Concentration of hqcdmn was $1 \times 10^{-5} \text{ mol L}^{-1}$ and the supporting electrolyte used was tetra-*n*-butylammonium hexafluorophosphate (0.05 mol L^{-1}). The cyclic voltammograms are characterized by one reduction peak and two oxidation peaks and are strongly dependent upon the scan rate. As

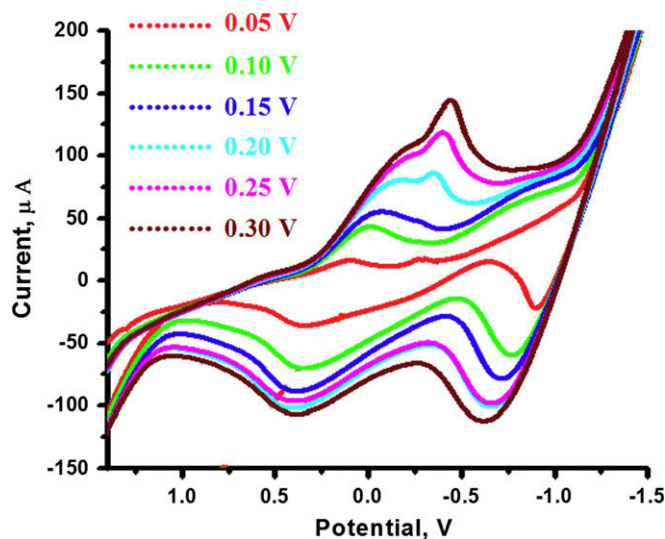


Fig. 7. Cyclic voltammograms of hqcdmn in 1:1 mixture of methanol–tetrahydrofuran with various scan rates.

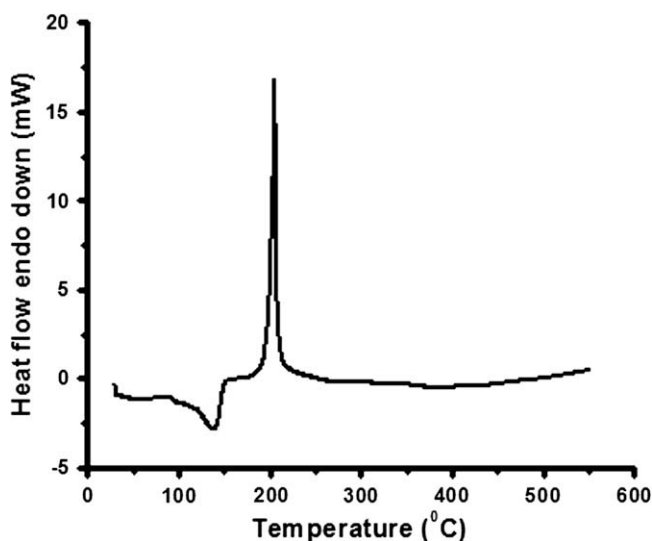


Fig. 8. DSC thermogram of hqcdmn in nitrogen.

the scan rate is increased a new cathodic peak is observed and its peak height increased with further increase in scan rate, which might be due to a self-protonation mechanism involving the proton transfer from the acidic iminol form to the basic reduction intermediate [42,43]. As the scan rate increases from 50 to 300 mV, the peak current ratio of the forward and reverse scans (i.e. I_{pc}/I_{pa}) increases from 1.10 to 2.40. This means that at the scan rate 50 mV,

the cyclic voltammogram is consistent with one electron transfer whereas at 300 mV it is in agreement with two electron transfers.

Fluorescent heteroaromatic compounds containing only imine nitrogen atoms (C=N) generally exhibiting less negative reduction potential compared to the analogous aromatic hydrocarbons and heteroaromatic rings with oxygen or sulphur atoms reported as good candidates for n-type semiconductors in organic electronics [44]. The half wave reduction potential of hqcdmn in methanol-THF ($1 \times 10^{-5} \text{ mol L}^{-1}$ at a scan rate 50 mV) is 0.112 V, which is comparatively more positive than that exhibited by pyrazine (-2.08 V) and quinoxaline (-1.62 V) [45] which indicates that it may be a better choice for n-type organic semiconductor.

3.7. Thermal analysis

The compound does not have a sharp melting point, but undergoes some phase change in the temperature range 175–180 °C and the colour of the compound changes to dark. The DSC thermogram of hqcdmn (Fig. 8) was recorded under nitrogen with a heating rate of 10 °C min^{-1} . The broad endothermic peak observed around 120 °C in the DSC thermogram may be due to the loss of water of crystallisation. There is a sharp exothermic peak at 204 °C, which may be due to the decomposition of the compound without melting.

The TG-DTA curves of hqcdmn in nitrogen atmosphere were recorded at a heating rate of 20 °C/min in the temperature range 40–800 °C and are shown in Fig. 9. The TG-DTA curves of hqcdmn in air atmosphere were recorded at a heating rate of 20 °C/min in the temperature range 40–500 °C and are shown in Fig. 9. We can

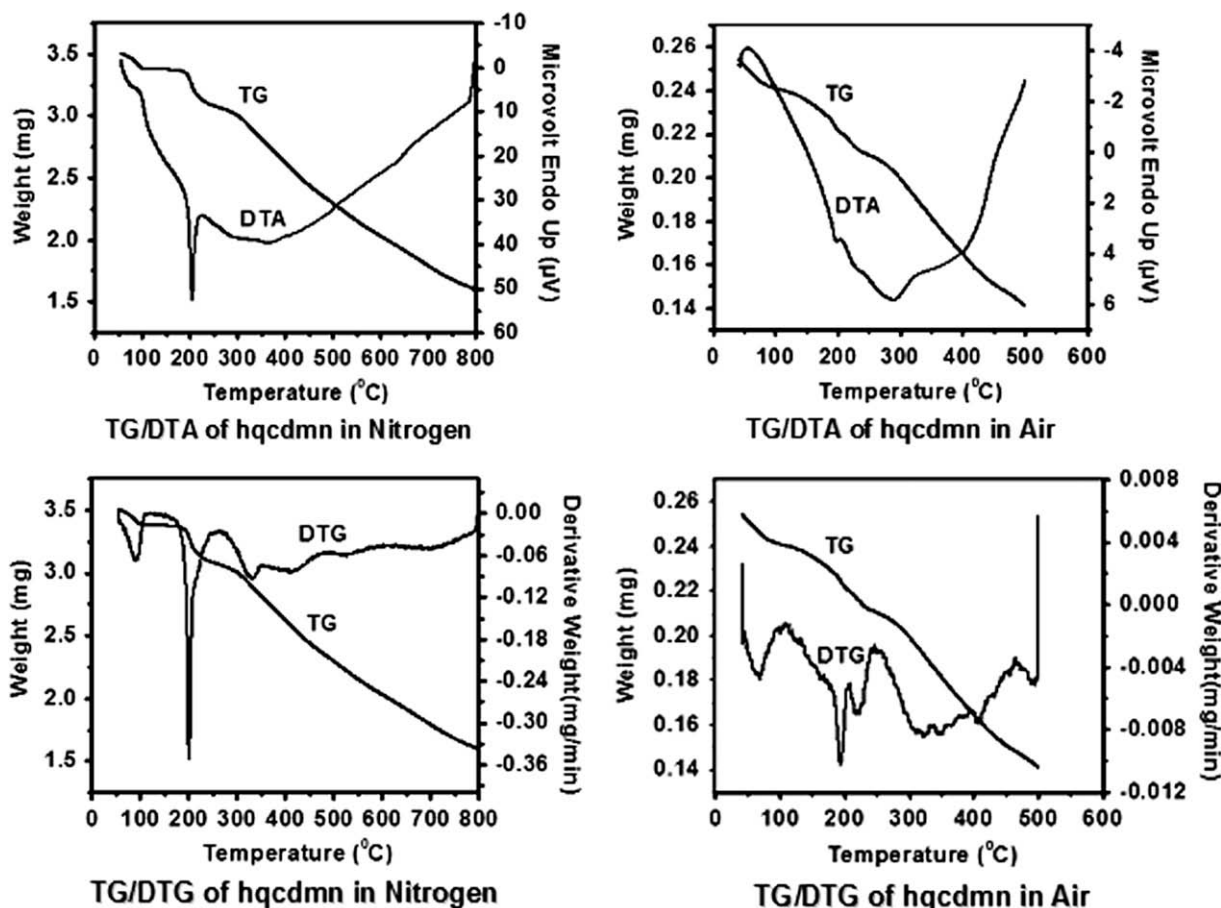


Fig. 9. TG-DTA curves of hqcdmn.

see somewhat similar thermal patterns in the nitrogen and air atmosphere. The initial weight loss in the TG–DTA–DTG thermograms in air and nitrogen may be due to the loss of water of crystallisation. The sharp exothermic peak around 200 °C in both cases may be due to the decomposition of the compound without melting. In both cases the decomposition is not completed at the specified range.

4. Conclusions

The synthesis and characterisation of a new Schiff base, hqcdmn, derived from 3-hydroxyquinoxaline-3-carboxaldehyde and 2,3-diaminomaleonitrile have been presented here. Like other 3-hydroxy derivatives of quinoxalines, the hqcdmn also exhibits prototropic tautomerism. It exhibits positive absorption and fluorescent solvatochromism and large stokes shift. The results of the UV–vis, fluorescence, CV and DSC studies suggest that the present compound is a suitable candidate for application as fluorescent and charge transport dyes. The dual emission of the fluorescent spectra and the results of cyclic voltammetric studies are in good agreement with the proton transfer in hqcdmn.

Acknowledgements

The authors thank Department of Science and Technology, India, for using the Sophisticated Analytical Instrumentation Facility (SAIF) at STIC, Cochin University of Science and Technology, Cochin for elemental analyses and DSC measurement. We also thank Dr. A. Ajayaghosh, NIIST, Trivandrum, Kerala for the ¹H NMR and ¹³C NMR spectra. V.D. thanks CSIR, India and S.M. thanks KSCSTE, Kerala for research fellowships.

References

- [1] Sonawane ND, Rangnekar DW. Synthesis and application of 2-styryl-6,7-dichlorothiazolo[4,5-*b*]quinoxaline based fluorescent dyes: part 3. *J Heterocycl Chem* 2002;39:303–8.
- [2] Brock ED, Lewis DM, Yousaf TI, Harper HH. The Proctor and Gamble Company; 1999. WO 9951688.
- [3] Katoh A, Yoshida T, Ohkanda J. Synthesis of quinoxaline derivatives bearing the styryl and phenylethynyl groups and application to a fluorescence derivatization reagent. *Heterocycles* 2000;52:911–20.
- [4] Ahmad AR, Mehta LK, Parrick J. Synthesis of some substituted quinoxalines and polycyclic systems containing the quinoxaline nucleus. *J Chem Soc Perkin Trans 1* 1996;2443–9.
- [5] Hirayama T, Yamasaki S, Ameku H, Ishi-i T, Thiemann T, Mataka S. Fluorescent solvatochromism of bipolar *N,N*-diphenylaminoaryl-substituted hexaazatriphenylenes, tetraazaphenanthrene, and quinoxalines. *Dyes Pigments* 2005;67:105–10.
- [6] Tsami A, Bunnagel TW, Farrell T, Scharber M, Choulis SA, Brabec CJ, et al. Alternating quinoxaline/oligothiophene copolymers – synthesis and unexpected absorption properties. *J Mater Chem* 2007;17:1353–5.
- [7] Wang P, Xie Z, Wong O, Lee CS, Wong N, Hung L, et al. New 1*H*-pyrazolo[3,4-*b*]quinoxaline derivatives as sharp green-emitting dopants for highly efficient electroluminescent devices. *Chem Commun* 2002;1404–5.
- [8] Thomas KRJ, Velusamy M, Lin JT, Tao Y-T, Chuen C-H. Chromophore-labeled quinoxaline derivatives as efficient electroluminescent materials. *Chem Mater* 2005;17(7):1860–6.
- [9] Kulkarni AP, Zhu Y, Jenekhe SA. Quinoxaline-containing polyfluorenes: synthesis, photophysics, and stable blue electroluminescence. *Macromolecules* 2005;38(5):1553–63.
- [10] Dailey S, Feast WJ, Peace RJ, Sage IC, Till S, Wood EL. Synthesis and device characterisation of side-chain polymer electron transport materials for organic semiconductor applications. *J Mater Chem* 2001;11:2238–43.
- [11] Fukuda T, Kanbara T, Yamamoto T, Ishikawa K, Takezo H, Fukuda A. Polyquinoxaline as an excellent electron injecting material for electroluminescent device. *Appl Phys Lett* 1996;68:2346–8.
- [12] Bettenhausen J, Greczmiel M, Jandke M, Strohhriegl P. Oxadiazoles and phenylquinoxalines as electron transport materials. *Synth Met* 1997;91:223–8.
- [13] O'Brien D, Weaver MS, Lidzey DG, Bradley DDC. Use of poly(phenyl quinoxaline) as an electron transport material in polymer light-emitting diodes. *Appl Phys Lett* 1996;69:881–3.
- [14] Carta A, Piras S, Loriga G, Paglietti G. Chemistry, biological properties and SAR analysis of quinoxalinones. *Mini-Rev Med Chem* 2006;6(11):1179–200.
- [15] Li X, Yang K-H, Li W-L, Xu W-F. Recent advances in the research of quinoxalinone derivatives. *Drugs Future* 2006;31(11):979.
- [16] Azqueta A, Arbillaga L, Pachon G, Cascante M, Creppy EE, Cerain AL. A quinoxaline 1,4-di-*N*-oxide derivative induces DNA oxidative damage not attenuated by vitamin C and E treatment. *Chem-Biol Interact* 2007;168(2):95–105.
- [17] Amiri H, Nekhotiaeva N, Sun J-S, Nguyen C-H, Grierson DS, Good L, et al. Benzoquinoxaline derivatives stabilize and cleave H-DNA and repress transcription downstream of a triplex-forming sequence. *J Mol Biol* 2005;351:776–83.
- [18] Kim S-H, Yoon S-H, Kim S-H, Han E-M. Red electroluminescent azomethine dyes derived from diaminomaleonitrile. *Dyes Pigments* 2005;64(1):45–8.
- [19] Shirai K, Matsuoka M, Fukunishi K. New syntheses and solid state fluorescence of azomethine dyes derived from diaminomaleonitrile and 2,5-diamino-3,6-dicyanopyrazine. *Dyes Pigments* 2000;47(1):107–15.
- [20] Kucybala Z, Pyszka I, Marciniak B, Hug GL, Paczkowski J. Azomethine dyes revisited. Photobleaching of azomethine dyes under photoreducing conditions. *J Chem Soc Perkin Trans 2* 1999;2147–54.
- [21] Jaung J, Matsuoka M, Fukunishi K. Dicyanopyrazine studies. Part V: syntheses and characteristics of chalcone analogues of dicyanopyrazine. *Dyes Pigments* 1998;40(1):11–20.
- [22] Cheeseman GWH, Werstuijk ESG. Quinoxaline chemistry. *Developments* 1963–1975. *Adv Heterocycl Chem* 1978;22:367–431.
- [23] Gein VL, Kataeva AV, Gein LF. Reaction of 1,5-diaryl-3-hydroxy-4-methylsulfonyl-3-pyrrolin-2-ones with urea, hydrazine, ethylenediamine, and *o*-phenylenediamine. *Chem Heterocycl Comp* 2007;43(11):1385–9.
- [24] Touzani R, Ben-Hadda T, Elkadiri S, Ramdani A, Maury O, Le Bozec H, et al. Solution, solid state structure and fluorescence studies of 2,3-functionalized quinoxalines: evidence for a π -delocalized keto-enamine form with N-H...O intramolecular hydrogen bonds. *New J Chem* 2001;25:391–5.
- [25] Gazit A, App H, McMahon G, Chen J, Levitzki A, Bohmer FD. Tyrphostins. 5. Potent inhibitors of platelet-derived growth factor receptor tyrosine kinase: structure–activity relationships in quinoxalines, quinolines, and indole tyrphostins. *J Med Chem* 1996;39(11):2170–7.
- [26] Mamedov VA, Kalinin AA, Gubaidullin AT, Isaikina OG, Litvinov IA. Synthesis and functionalization of 3-ethylquinoxalin-2(1*H*)-one. *Russ J Org Chem* 2005;41(4):599–606.
- [27] Bozdyreva KS, Aliev ZG, Masliviets AN. Five-membered 2,3-dioxo heterocycles: LVII. Recyclization of 3-pivaloylpyrrolo[1,2-*a*]quinoxaline-1,2,4(5*H*)-triones by the action of *o*-phenylenediamine. Crystalline and molecular structure of 3-[3,3-dimethyl-2-oxo-1-(3-oxo-3,4-dihydroquinoxalin-2-yl)butyl]-1-phenylquinoxalin-2(1*H*)-one. *Russ J Org Chem* 2008;44(4):607–11.
- [28] Mamedov VA, Kalinin AA, Gubaidullin AT, Rizvanov IKh, Chernova AV, Doroshkina GM, et al. Fused nitrogen-containing heterocycles: IV. 3-Benzoyl-2-oxo-1,2-dihydroquinoxaline hydrazones and flavazoles derived therefrom. *Russ J Org Chem* 2003;39(1):131–40.
- [29] Mashevskaya IV, Tolmacheva IA, Voronova EV, Odegova TF, Aleksandrova GA, Goleneva AF, et al. A comparative study of the antimicrobial activity of some quinoxalines, 1,4-benzoxazines, and aza-analogs. *Pharma Chem J* 2002;36(2):86–8.
- [30] Kotb ER, Anwar MA, Soliman MS, Salama MA. Synthesis and reactions of some novel quinoxalines for anticancer evaluation. *Phosphorus Sulfur Silicon Relat Elem* 2007;182(5):1119–30.
- [31] Bellamy LJ. The infra-red spectra of complex molecules. London: Methuen; 1956.
- [32] Mamedov VA, Kalinin AA, Azancheev NM, Levin YA. Fused nitrogen-containing heterocycles: III. 4-Oxo-1-phenyl-4,5-dihydroimidazo[1,5-*a*]quinoxalines. A retrosynthetic approach. *Russ J Org Chem* 2003;39(1):125–30.
- [33] Mamedov VA, Kalinin AA, Gubaidullin AT, Nurkhametova IZ, Litvinov IA, Levin YA. 3-Aryl-1-imino-4-oxo-4,5-dihydrothiazolo[3,4-*a*]quinoxalines. Retrosynthetic approach. *Chem Heterocycl Comp* 1999;35(12):1459–73.
- [34] Mamedov VA, Saifina DF, Berdnikov EA, Rizvanov IKh. Fused polycyclic nitrogen containing heterocycles 16. Selenazolo[3,4-*a*] and thiazolo[3,4-*a*]quinoxalin-4(5*H*)-ones. *Russ Chem Bull Int Ed* 2007;56(10):2127–30.
- [35] Seok YJ, Yang KS, Kim ST, Huh WK, Kang SO. Characterization of quinoxaline derivatives of dehydro-D-erythroascorbic acid. *J Carbohydr Chem* 1996;15(9):1085–96.
- [36] Ahmed M, Khanl ZH. Electronic absorption spectra of benzoquinone and its hydroxy substituents and effect of solvents on their spectra. *Spectrochim Acta A* 2000;56(5):965–81.
- [37] Hao Y, Xu B, Gao Z, Wang H, Zhou H, Liu X. Optical properties, electronic energy level structure and electro-luminescent characteristics of salicylaldehyde anil zinc. *J Mater Sci Technol* 2006;22(2):225–9.
- [38] Kolehmainen E, Osmialowski B, Nissinen M, Kauppinen R, Gawinecki R. Substituent and temperature controlled tautomerism of 2-phenylacetylpyridine: the hydrogen bond as a configurational lock of (Z)-2-(2-hydroxy-2-phenylvinyl)pyridine. *J Chem Soc Perkin Trans 2* 2000:2185–91.
- [39] Katritzky AR, Ghiviriga I, Oniciu DC, O'Ferrall RAM, Walsh SM. Study of the enol–enaminone tautomerism of α -heterocyclic ketones by deuterium effects on ¹³C chemical shifts. *J Chem Soc Perkin Trans 2* 1997:2605–8.
- [40] Sasirekha V, Umadevi M, Ramakrishnan V. Solvatochromic study of 1,2-dihydroxyanthraquinone in neat and binary solvent mixtures. *Spectrochim Acta A Mol Biomol Spectrosc* 2008;69(1):148–55.
- [41] Vollmer F, Rettig W, Birckner E. Photochemical mechanisms producing large fluorescence stokes shifts. *J Fluoresc* 1994;4(1):65–9.

- [42] Isse AA, Abdurahman AM, Vianello E. Self-protonation mechanism in the electroreduction of hydroxyimines. *J Chem Soc Perkin Trans 2* 1996:597–600.
- [43] Isse AA, Gennaro A, Vianello E. Electrochemical reduction of Schiff base ligands H₂salen and H₂salophen. *Electrochim Acta* 1997;42:2065–71.
- [44] Tonzola CJ, Alam MM, Kaminsky W, Jenekhe SA. New n-type organic semiconductors: synthesis, single crystal structures, cyclic voltammetry, photophysics, electron transport, and electroluminescence of a series of diphenylanthrazolines. *J Am Chem Soc* 2003;125(44):13548–58.
- [45] Mancilha FS, DaSilveira Neto BA, Lopes AS, Moreira Jr PF, Quina FH, Gonçalves RS, et al. Are molecular 5,8-extended-quinoxaline derivatives good chromophores for photoluminescence applications? *Eur J Org Chem* 2006:4924–33.